Inorganica Chimica Acta, *207* (1993) 241–252

Bis(trithiacyclononane)metal(II) compounds and Jahn–Teller distortions from octahedral geometry, electrochemistry, spectroscopy, and crystal structures of the copper bis(tetrafluoroborate) bis(acetonitrile) complex at 177 K and the cadmium bis(tetrafluoroborate) and copper bis(tetrafluoroborate) bis(nitromethane) complexes at 300 K

Richard S. Glass, L. Kraig Steffen, Dale D. Swanson, George S. Wilson*
Department of Chemistry, The University of Arizona, Tucson, AZ 85721 (USA)

René de Gelder, Rudolf A. G. de Graaff and Jan Reedijk
Department of Chemistry, Gorlaeus Laboratories, Leiden University, P.O. Box 9502, 2300 RA Leiden (Netherlands)

(Received October 11, 1991; revised January 20, 1993)

Abstract

The structures and the EPR spectra are described of compounds with formula $M(ttcn)_2(A)_2$, with $A = BF_4^-$; M = Cu, Cd, Fe and the Cu(II)-doped Cd(II) and Fe(II) compounds. Single crystal structures are described for the copper compound $Cu(ttcn)_2(BF_4)_2(MeCN)_2$ (**1**) at low temperature, and for the cadmium compound $Cd(ttcn)_2(BF_4)_2(MeNO_2)_2$ (**2**) and copper compound $Cu(ttcn)_2(BF_4)_2(MeNO_2)_2$ (**3**) at room temperature. Compound **1** crystallizes in the space group $P2_1/c$ with $a = 20.695(2)$, $b = 14.944(1)$, $c = 8.864(1)$ Å, $\beta = 90.797(8)°$ and $Z = 4$. The unit cell contains two crystallographically independent Cu ions, each at a crystallographic inversion center, which are structurally almost identical. The copper ion with the CuS_6^{2+} chromophore appears to be nearly octahedral, just as found earlier for the room temperature structure. Relevant Cu–S distances are for Cu(A): 2.407, 2.419 and 2.458 and for Cu(B): 2.407, 2.428 and 2.461 Å. Compound **2** also crystallized in the space group $P2_1/c$ with $a = 10.314(2)$, $b = 15.138(2)$, $c = 9.461(2)$ Å, $\beta = 99.39(1)°$ and $Z = 2$. The Cd(II) ion is octahedrally surrounded by six S atoms at almost equal distances varying from 2.649 to 2.663 Å. Compound **3** crystallizes in the space group *Pbca* with $a = 19.746(2)$, $b = 15.422(2)$, $c = 9.227(1)$ Å and $Z = 4$. The copper ion occupies a crystallographic inversion center. The copper ion is significantly distorted from an octahedral arrangement of the six coordinated sulfur atoms with Cu–S distances ranging from 2.343(2) to 2.504(2) Å. Cyclic voltammetric studies on $Cu(ttcn)_2^{2+}$ in aqueous buffer at pH 3 show a reversible one-electron reduction with $E^{0\prime} = 0.408(1)$ V versus AgCl/Ag reference. EPR spectra were recorded of the pure copper compound acetonitrile solvate, as well as of Cu(II) dopes in the isomorphous Fe(II) and Cd(II) compounds. The results indicate that in the case of the undiluted copper compound only a single signal ($g = 2.06$) is observed even down to 4 K, thereby not providing any evidence of a Jahn–Teller splitting. However, Cu(II) dopes in the isomorphous, diamagnetic Fe(II) compound show anisotropic signals below 100 K, with values for $g_\parallel$ and $g_\perp$ of 2.113 and 2.027, respectively ($A_\parallel = 153$ G). At room temperature a complex spectrum of isotropic and anisotropic lines is observed. Dopes in the corresponding Cd compounds show well-resolved spectra, with parameters similar to the Fe(II)-doped species. Heat capacity measurements on compound **3** show no phase transition in the temperature range 1.2–300 K. Such measurements on compound **1** show phase transitions near 90 and 150 K.

Introduction

During the last few years a large variety of compounds with the tridentate ligand 1,4,7-trithiacyclononane (abbreviated ttcn) has been reported and characterized by spectroscopic and structural methods [1–26]. It appears that for most metal ions regular, octahedrally based geometries are found. Only with metal ions like Pd(II) [5, 7, 19] and Pt(II) [8], that prefer square-planar geometries, or metal ions like Cu(I) [14, 23] and Au(I) [21], that prefer tetrahedral geometries, are deviations from regular octahedral structures found. In the case of Co(II), two different compounds have been reported in the literature: one having one molecule of nitromethane in the lattice [6], the other having two

---

*Present address: Department of Chemistry, University of Kansas, Lawrence, KS 66045, USA.

0020-1693/93/$6.00

© 1993 – Elsevier Sequoia. All rights reserved

solvent molecules [1]. The first compound appears to have an almost undistorted octahedral geometry; whereas the second compound, differing only in one solvent molecule, has a significantly distorted geometry, ascribed to a Jahn–Teller distortion [6].

Surprisingly, regular octahedral geometry was also found [1] for Cu(II), despite the known preference for Jahn–Teller distortions in cases of trigonal and octahedral geometry. However because many copper compounds show temperature dependent geometric distortions, and single copper ions in a host lattice of regular symmetry may exhibit interesting spectroscopic properties, a study of low-T spectra and structures of pure copper and doped copper compounds was undertaken. Therefore the X-ray structure of the $Cu(ttcn)_2(BF_4)_2(MeCN)_2$ salt was redetermined at low temperature (−156 °C), and dopes of Cu(II) in the Cd(II) and Fe(II) isomorphous compounds were studied spectroscopically. During the course of this investigation a paper appeared describing the solution and frozen-solution EPR of $Cu(ttcn)_2(ClO_4)_2$ [27]. The powder spectrum of this compound is reported to be complicated, due to exchange narrowing effects [27]. To fully understand the dopes in the Cd lattice, the structure of the Cd compound (as its BF_4 salt and nitromethane crystallized product) was also determined. The X-ray structure of the $Cu(ttcn)_2(BF_4)_2(MeNO_2)_2$ salt was determined at room temperature.

Experimental

Starting material

Most solvents, metal salts and starting reagents were commercially available and used without further purification.

The ligand 1,4,7-trithiacyclononane (ttcn) was obtained from Aldrich Chemical Co., Milwaukee, WI and used as received.

Synthesis of $Cd(ttcn)_2(BF_4)_2(MeNO_2)_2$

A sample of ttcn (63.8 mg, 0.35 mmol) was dissolved in ethanol (10 ml) by gentle heating. Cadmium(II) tetrafluoroborate (60 mg, 0.18 mmol) was added to the warm ethanol solution. A white precipitate formed as the ethanol cooled. The precipitate was filtered and washed with diethyl ether (≈3 ml) and allowed to dry to give a white solid (120 mg, 95% yield). IR (KBr): 2988, 1649, 1424, 1289, 1053 (s, BF_4^-), 929, 880, 824, 521 cm^{-1}. *Anal.* Calc. for $C_{12}H_{24}S_6CdB_2F_8(CH_3NO_2)_{1/2}$: C, 22.17; H, 3.80; S, 28.41; Cd, 16.60. Found: C, 21.94; H, 3.81; S, 28.82; Cd, 16.77%. Recrystallization by vapor diffusion of diethyl ether into a nitromethane solution of this complex yielded small translucent white crystals suitable for X-ray structure analysis, which contain two molecules of nitromethane per $Cd(ttcn)_2(BF_4)_2$ unit but lose solvent on standing at room temperature or on drying under reduced pressure (elemental analysis is on dried sample).

Synthesis of $Cu(ttcn)_2(BF_4)_2(MeNO_2)_2$ and $Cu(ttcn)_2(BF_4)_2(MeCN)_2$

A solution of copper(II) tetrafluoroborate hydrate (0.72 g, 2.6 mmol) in absolute ethanol (20 ml) was added to a solution of ttcn (0.93 g, 5.2 mmol) in absolute ethanol (20 ml). A brown solution formed immediately followed by precipitation of a brown solid. The precipitate was filtered off and washed with absolute ethanol to yield 1.24 g of a fine brown powder. This procedure is the same as reported by Setzer *et al.* [1] and was used to make several batches of the complex which were recrystallized in the following ways.

Recrystallization of the crude product by vapor diffusion of diethyl ether into a nitromethane solution yielded small translucent brown crystals of $Cu(ttcn)_2(BF_4)_2(MeNO_2)_2$ used for X-ray diffraction analysis. IR (KBr): 2975, 1555, 1445, 1287, 1056 (s, BF_4^-), 932, 893, 820, 669, 520 cm^{-1}. *Anal.* Calc. for $C_{12}H_{24}S_6CuB_2F_8$: C, 24.11; H, 4.05; S, 32.18; Cu, 10.63. Found: C, 24.05; H, 3.88; S, 32.46; Cu, 10.81%. This analysis is on a dried sample.

Recrystallization of the crude product by vapor diffusion of diethyl ether into an acetonitrile solution of the crude complex yielded brown crystals whose IR was identical with those reported for the copper complex with acetonitrile as the solvent of recrystallization [1]. Solvent of crystallization is lost on standing at room temperature or on drying under reduced pressure.

Synthesis of Cu-doped $Cd(ttcn)_2(BF_4)_2(MeNO_2)_2$

A sample of $Cd(ttcn)_2(BF_4)_2(MeNO_2)_2$ (79 mg, 0.1 mmol) and $Cu(ttcn)_2(BF_4)_2(MeNO_2)_2$ (5.2 mg, 0.008 mmol) was dissolved in nitromethane (3 ml) and diethyl ether was allowed to diffuse in overnight. Pale brown crystals were obtained. Inductively coupled plasma atomic emission (ICP-AES) analysis of this sample showed 0.61% by weight copper.

Synthesis of Cu-doped $Fe(ttcn)_2(BF_4)_2$

A sample of $Fe(ttcn)_2(BF_4)_2$ was prepared in a similar manner to that reported by Wieghardt *et al.* [3] for the preparation of $Fe(ttcn)_2(PF_6)_2$. The synthesis of Cu-doped $Fe(ttcn)_2(BF_4)_2$ was accomplished by using the same procedure as that reported above for the synthesis of Cu-doped $Cd(ttcn)_2(BF_4)_2(MeNO_2)_2$ except that $Fe(ttcn)_2(BF_4)_2$ was substituted for $Cd(ttcn)_2(BF_4)_2(MeNO_2)_2$.

Spectroscopic and instrumental techniques

IR spectra (4000–180 cm^{-1}) were recorded on a Perkin-Elmer PE380 instrument, using KBr pellets and nujol mulls between NaCl or polyethylene discs. EPR spectra of powdered samples were measured on a Varian E-3 EPR spectrometer using a 9.5 GHz microwave bridge, at ambient temperature and liquid nitrogen temperature. Spectra at 4.2 K were recorded at X-band frequencies with the above mentioned equipment, and at Q-band frequencies using Varian E9 equipment at the University of Amsterdam. Elemental analyses were performed at Galbraith Laboratories, Inc., Knoxville, TN.

Crystal structure determination of the copper compound 1

The intensities were measured at 117 K on an Enraf-Nonius CAD4 diffractometer using a parallelepiped crystal of dimensions 0.20×0.30×0.50 mm. Crystals suitable for X-ray analysis were obtained from the reaction mixture, without further crystallization. Detailed information on the data collection and processing and the results of the refinement are given in Table 1. The position of the copper atom was obtained from a sharpened Patterson map and the other non-hydrogen atoms were found using the iterative Fourier program AUTOFOUR [28]. The positions of the hydrogen atoms were obtained from difference Fourier synthesis.

Conventional block-diagonal least-squares using anisotropic temperature factors for the non-hydrogen atoms, rapidly converged to a final R_w value of 0.0382 (R=0.0333) based on 3465 reflections with $I>2\sigma(I)$. The hydrogen atoms were refined using one overall B factor (2.52 Å^3) and riding on the parent atoms. The e.s.d.s of the distances and angles given in this paper were calculated based on an estimate of the variance-covariance matrix obtained from a final full-matrix cycle of least-squares. Table 2 contains a list of the coordinates of the heavy atoms and B_{eq} obtained from the trace of the U tensor. See also 'Supplementary material'.

TABLE 1. Crystal data and details of measurement and structure analysis and refinement of Cu(ttcn)$_2$(BF$_4$)$_2$(MeCN)$_2$ (**1**) at 117 K

Formula	$CuC_{16}H_{30}N_2S_6B_2F_8$
Molecular weight	679.943
Crystal system	monoclinic
Space group	$P2_1/c$
a (Å)	20.695(2)
b (Å)	14.944(1)
c (Å)	8.864(1)
β (°)	90.797(8)
V (Å^3)	2.6854(1)
Z	4
D_{calc} (g cm^{-3})	1.68
λ(Mo Kα) (Å)	0.71073
Scan mode	1/ω scan
Scan range	$2<\theta<27.5$
No. independent data collected	6392
No. data with $I>2\sigma(I)$	3465
Weighting scheme	$w=(1/\sigma)2$
R	0.0333 (3465 reflections)
R_w	0.0382 (3465 reflections)
R_{int}	0.0252

TABLE 2. Fractional coordinates[a] for the cations Cu(ttcn)$_2$$^{2+}$ and the anion and solvent molecule for **1** at 117 K

Atom	x	y	z	B_{iso}
Cu(A)	0	0	0	1084(14)
S(1A)	−252(5)	2238(7)	−28049(12)	194(2)
S(2A)	10856(5)	5942(7)	2122(12)	180(2)
S(3A)	4713(5)	−14630(7)	−2717(12)	167(2)
C(1A)	−681(2)	−551(3)	−3258(5)	185(9)
C(2A)	1272(1)	483(3)	2251(5)	172(9)
C(3A)	1517(1)	−330(2)	−656(5)	168(8)
C(4A)	1336(1)	−1255(3)	−88(5)	173(9)
C(5A)	266(1)	−1918(2)	1591(5)	168(9)
C(6A)	−406(1)	1320(2)	−2966(5)	167(8)
N(A)	962(1)	2215(2)	−4097(5)	328(10)
C(7A)	2055(2)	1794(3)	−2890(6)	360(13)
C(8A)	1441(2)	2029(2)	−3571(5)	200(9)
B(A)	3149(2)	1166(3)	464(5)	174(10)
F(1A)	30009(10)	5953(13)	−7482(23)	309(6)
F(2A)	31465(10)	20318(13)	−625(35)	363(6)
F(3A)	26831(10)	10642(20)	15820(23)	368(6)
F(4A)	37595(10)	9609(13)	10554(23)	274(6)
Cu(B)	500	0	500	1171(14)
S(1B)	50668(5)	−2994(7)	22826(12)	199(2)
S(2B)	60211(5)	8336(7)	48314(12)	213(2)
S(3B)	56360(5)	−13403(7)	54668(12)	176(2)
C(1B)	5624(2)	588(3)	1775(5)	201(9)
C(2B)	6216(2)	699(3)	2812(5)	203(9)
C(3B)	6544(1)	20(3)	5787(5)	178(8)
C(4B)	6462(1)	−940(3)	5286(5)	164(9)
C(5B)	5484(1)	−1886(2)	3635(5)	172(9)
C(6B)	5565(1)	−1302(2)	2224(3)	153(8)
N(B)	−4135(1)	2907(2)	3445(5)	358(10)
C(7B)	−2962(2)	3356(3)	4110(6)	323(13)
C(8B)	−3622(2)	3101(2)	3732(5)	215(9)
B(B)	−1875(2)	3829(3)	−597(5)	204(10)
F(2B)	−19873(10)	34708(13)	8530(23)	311(6)
F(1B)	−18618(10)	47472(13)	−4949(23)	367(7)
F(3B)	−23544(10)	35801(13)	−16244(35)	433(7)
F(4B)	−12875(10)	35333(20)	−11299(23)	431(7)

[a] Cu(A), Cu(B), S(A), S(B)×10^5; ×10^4 for all others.
[b] Equivalent isotropic thermal parameters Å^2×10^3 for Cu(A) and Cu(B) and Å^2 for all others.

Crystal structure of the cadmium compound 2

A colorless, trapezoidal, parallelepiped crystal, prepared by vapor diffusion as described above, having approximate dimensions of 0.55×0.18×0.28 mm was mounted in a glass capillary. The intensities were measured at room temperature using a Syntex P2$_1$ diffractometer. Detailed information on the data collection and processing and the results of the refinement are given in Table 3. All calculations were performed on

TABLE 3. Crystal data and details of measurement and structural analysis and refinement of $Cd(ttcn)_2(BF_4)_2(MeNO_2)_2$ (**2**) and $Cu(ttcn)_2(BF_4)_2(MeNO_2)_2$ (**3**) at room temperature (23 °C ± 1)

Formula	$CdC_{14}H_{30}O_4N_2S_6B_2F_8$	$CuC_{14}H_{30}O_4N_2S_6B_2F_8$
Molecular weight	768.80	719.91
Crystal system	monoclinic	orthorhombic
Space group	$P2_1/c$	$Pbca$
a (Å)	10.314(2)	19.746(2)
b (Å)	15.138(2)	15.422(2)
c (Å)	9.461(2)	9.227(1)
β (°)	99.39(1)	
V (Å^3)	1457.3	2810.0
Z	2	4
D_{calc} (g cm^{-3})	1.75	1.68
λ(Mo Kα) (Å)	0.71073	0.71073
Scan mode	$2\theta/\theta$	$2\theta/\theta$
Maximum 2θ (°)	50.0	50.0
No. independent data collected	4273	2486
No. data with $I > 3\sigma(I)$	2870	1098
Weighting scheme	$w = 4F^2/\sigma^2(F^2)w$	$w = 4F_o^2/\sigma^2(F_o^2)$
μ_λ (cm^{-1})	12.3	12.8
R	0.053	0.053
R_w	0.068	0.061

a PDP-11/34 computer using SDS-PLUS [29]. The position of the cadmium atom was obtained from a Patterson map and the remaining non-hydrogen atoms were located in succeeding difference Fourier syntheses. Hydrogen atoms were included at idealized positions and, in subsequent refinements, they were constrained to ride on the atom to which they are bonded with fixed isotropic thermal parameters. Full-matrix least-squares refinement using anisotropic temperature factors for the non-hydrogen atoms converged to a final R_w value of 0.068 ($R = 0.053$) based on 2870 reflections with $I > 3\sigma(I)$. The standard deviation of an observation of unit weight was 3.19. The highest peak in the final difference Fourier had a height of 0.91 e^{-1}/Å^3 with an estimated error based on $\sigma(F)$ of 0.13. The BF_4 anion and solvent are not well-behaved as evidenced by their large thermal parameters and the large residual electron density in the final difference map. Table 4 lists the coordinates of the non-hydrogen atoms and B_{eq}. See also 'Supplementary material'.

TABLE 4. Positional and thermal parameters for $Cd(ttcn)_2(BF_4)_2(MeNO_2)_2$

Atom	x	y	z	B (Å^2)[a]
Cd	0.000	0.000	0.000	3.617(8)
S1	−0.0050(1)	−0.03821(9)	0.2739(1)	4.14(2)
S2	0.1274(1)	−0.15236(8)	0.0060(1)	4.09(2)
S3	0.2362(1)	0.06248(9)	0.1044(1)	4.80(3)
C1	0.0834(5)	−0.1420(3)	0.2957(5)	4.5(1)
C2	0.0684(6)	−0.1985(3)	0.1590(6)	4.8(1)
C3	0.2950(5)	−0.1208(4)	0.0770(7)	5.4(1)
C4	0.3318(5)	−0.0272(5)	0.0464(7)	5.7(1)
C5	0.2471(6)	0.0433(4)	0.2951(5)	5.4(1)
C6	0.1166(6)	0.0418(4)	0.3495(5)	5.3(1)
B	0.3514(6)	−0.1061(5)	0.6534(7)	4.7(1)
F1	0.3705(6)	−0.1382(6)	0.5309(6)	13.5(2)
F2	0.2271(5)	−0.1066(5)	0.6650(8)	13.4(2)
F3	0.3900(9)	−0.0263(5)	0.674(1)	18.0(3)
F4	0.4173(9)	−0.1466(7)	0.7524(9)	24.0(3)
O1	0.1855(6)	0.2054(6)	0.587(1)	14.6(3)
O2	0.2785(9)	0.1983(7)	0.7980(7)	23.3(3)
N	0.2815(6)	0.1999(4)	0.6823(7)	8.1(2)
C	0.4028(7)	0.1927(6)	0.6333(9)	7.8(2)

[a]Anisotropically refined atoms are given in the form of the isotropic equivalent thermal parameter defined as: $8\pi^2(U_{11}+U_{22}+U_{33})/3$.

Crystal structure of the copper compound 3

A dark rectangular crystal of $Cu(ttcn)_2(BF_4)_2(MeNO_2)_2$ having approximate dimensions of 0.55 × 0.05 × 0.20 mm was mounted in a glass capillary. The intensities were measured at room temperature using a Syntex $P2_1$ diffractometer. Detailed information on the data collection and processing and the results of the refinement are given in Table 3 [29]. The structure was solved using the Patterson heavy-atom method which revealed the position of the Cu atom at crystallographic inversion centers. The remaining atoms were located in succeeding difference Fourier syntheses. Hydrogen atoms were included in the refinement but constrained to ride on the atom to which they are bonded. Full-matrix least-squares refinement led to a final R_w value of 0.061 ($R = 0.053$) based on 1098 reflections with $I > 3\sigma(I)$. The standard deviation of an observation of unit weight was 2.29. There were three correlation coefficients greater than 0.50. The highest correlation coefficient was 0.656 which was between

TABLE 5. Positional and thermal parameters for $Cu(ttcn)_2(BF_4)_2(MeNO_2)_2$

Atom	x	y	z	B (Å^2)
Cu	0.000	0.000	0.000	2.63(3)
S1	−0.0043(2)	−0.0349(2)	0.2649(3)	4.09(5)
S2	0.1107(1)	0.0508(2)	0.0345(3)	3.42(5)
S3	−0.0483(1)	0.1474(2)	0.0361(3)	3.70(6)
C1	0.0637(6)	0.0397(7)	0.317(1)	4.6(3)
C2	0.1277(5)	0.0356(7)	0.227(1)	4.2(2)
C3	0.1572(5)	−0.0360(6)	−0.054(1)	4.0(2)
C4	−0.1385(4)	0.1271(6)	0.010(1)	4.2(2)
C5	−0.0233(5)	0.1939(6)	−0.134(1)	3.6(2)
C6	0.0360(5)	−0.1421(5)	0.268(1)	3.8(2)
B	0.3199(6)	0.1157(8)	0.062(1)	3.8(3)
F1	0.3090(6)	0.0328(6)	0.085(1)	13.3(3)
F2	0.3115(4)	0.1352(6)	−0.0742(7)	9.8(2)
F3	0.2810(6)	0.1528(8)	0.150(1)	20.0(4)
F4	0.3836(5)	0.1256(7)	0.106(1)	11.7(3)
C7	0.1975(6)	0.1754(7)	0.717(1)	6.0(3)
N	0.1524(6)	0.1969(6)	0.602(1)	7.1(3)
O1	0.1744(9)	0.1801(6)	0.482(1)	14.4(5)
O2	0.1029(5)	0.2380(8)	0.623(2)	14.4(4)

Anisotropically refined atoms are given in the form of the isotropic equivalent displacement parameter defined as: $(4/3)[a^2B(1,1)+b^2B(2,2)+c^2B(3,3)+ab(\cos\gamma)B(1,2)+ac(\cos\beta)B(1,3)+bc(\cos\alpha)B(2,3)]$.

two of the thermal parameters of atom F3. All three are intraatomic correlations. The highest peak in the final difference Fourier had a height of 0.55 $e^{-1}/Å^3$ with an estimated error based on ΔF of 0.10; the minimum negative peak had a height of -0.34 $e^{-1}/Å^3$ with an estimated error based on ΔF of 0.10. Plots of $\Sigma w(|F_o|-|F_c|)^2$ versus $|F_o|$, reflection order in data collection, $(\sin\theta)/\lambda$, and various classes of indices showed no unusual trends. Table 5 lists the coordinates of the non-hydrogen atoms and B_{eq} values. See also 'Supplementary material'.

Electrochemical measurements

Cyclic voltammetric measurements were made with a computer-controlled data acquisition system described previously [30] and with a Cypress Systems (Lawrence, KS) model CYSY-1H. Measurements were carried out in aqueous tetrafluoroboric acid pH 3 with 0.1 M $NaBF_4$ as supporting electrolyte. The reference electrode was AgCl/Ag NaCl(sat) and the working electrode was either Pt (1.2 cm^2) or glassy carbon (0.071 cm^2). The cyclic voltammetric data were analyzed using a PC-based computation and curve fitting system [31]. A Princeton Applied Research model 373 digital coulometer was used for controlled potential coulometry along with a Pine Instruments PIR rotator and DT6 rotating disk electrode.

Formation constants

Formation constants were determined by titrating an aqueous solution of 1.10×10^{-4} M in $Cu(BF_4)_2$, with an ethanolic solution 6.94×10^{-3} M in ttcn. Spectra were recorded on a Varian Cary model 219 spectrophotometer with computer interface for on-line data acquisition. An Orion model 94-29 cupric ion electrode was used to monitor free Cu^{2+} concentration during the titration.

Results and discussion

Description of the structure of $Cu(ttcn)_2(BF_4)_2(MeCN)_2$

Coordination bond distances and angles of the cations are given in Table 6. A drawing of the cation $Cu(ttcn)_2^{2+}$ (A), with the atomic numbering, is given in Fig. 1. The other cation is very similar in geometry. The ttcn ligand acts as a tridentate ligand to the copper ions, occupying a face of the octahedron.

The Cu–S distances (average 2.43 Å) are comparable to the distances found in similar compounds [32]. A comparison of several ttcn structures is given in Table 7. The most surprising outcomes of the structure determination at low temperature are: (i) The geometry of the CuS_6 chromophore remains essentially octahedral (to be sure the CuS_6 geometry is not precisely octahedral as revealed by the small but real variation in the Cu–S distances and S–Cu–S bond angles. Another way to picture the modest distortion is by viewing the CuS_6 chromophore down the pseudo C_3 axis through the copper atom and perpendicular to the two parallel planes each one defined by the three sulfur atoms in the same ttcn ligand. In an ideal octahedron the dihedral angle between the sulfur atom of one ttcn ligand and the center of these planes and either *cis* sulfur atom on the other ligand and the centers of the two planes is 60° as illustrated in Fig. 2. However, in $Cu(ttcn)_2^{2+}$ (A) these angles differ from 60° by 0.8–2.8° and in (B) they differ by 0.2–2.5°); contrary to what one would expect for a system sensitive to Jahn–Teller distortion*. (ii) As a result of a phase transition somewhere between 300 and 117 K the molecular packing changes but the two crystallographically independent Cu(II) sites have statistically identical geometry. On cooling the Cu–S bonds (on average) have decreased from 2.435 to 2.430 Å. The heat capacity measurements show a phase transition around 150 K and another between 50 and 100 K. The phase transition around 150 K is consistent with the X-ray crystallographic structure studies. At

---

*It has been suggested [33] that the X-ray structure of this complex at room temperature is a time-averaged structure. It is surprising that this must still be the case at 117 K. Although Jahn–Teller distortion is not manifested in the overall geometry of the CuS_6 coordination sphere, analysis of the thermal parameters show Jahn–Teller radii indicative of a strong Jahn–Teller effect [34].

TABLE 6. Bond lengths (Å) and bond angles (°) in $Cu(ttcn)_2(BF_4)_2(MeCN)_2$

Bond distances (Å)[a]			
Cu(A)–S(1A)	2.459(1)	Cu(B)–S(1B)	2.408(1)
Cu(A)–S(2A)	2.4205(9)	Cu(B)–S(2B)	2.459(1)
Cu(A)–S(3A)	2.4070(9)	Cu(B)–S(3B)	2.4277(9)
S(1A)–C(1A)	1.823(4)	S(1B)–C(1B)	1.815(4)
S(1A)–C(6A)	1.823(3)	C(6B)–S(1B)	1.819(3)
S(2A)–C(2A)	1.814(4)	S(2B)–C(2B)	1.816(4)
S(2A)–C(3A)	1.814(3)	C(3B)–S(2B)	1.820(4)
S(3A)–C(4A)	1.820(3)	C(4B)–S(3B)	1.821(3)
S(3A)–C(5A)	1.811(4)	C(5B)–S(3B)	1.811(3)
C(1A)–C(2A)	1.517(5)	C(1B)–C(2B)	1.519(5)
C(3A)–C(4A)	1.516(5)	C(4B)–C(3B)	1.507(5)
C(5A)–C(6A)	1.516(5)	C(5B)–C(6B)	1.516(5)
N(A)–C(8A)	1.121(5)	N(B)–C(8B)	1.126(5)
C(7A)–C(8A)	1.437(6)	C(7B)–C(8B)	1.450(6)
B(A)–F(1A)	1.386(4)	B(B)–F(1B)	1.376(5)
B(A)–F(2A)	1.372(4)	B(B)–F(2B)	1.391(5)
B(A)–F(3A)	1.386(4)	B(B)–F(3B)	1.377(5)
B(A)–F(4A)	1.392(4)	B(B)–F(4B)	1.378(4)
S(1A)–Cu(A)–S(2A)	91.86(3)	S(1B)–Cu(B)–S(2B)	88.55(3)
S(1A)–Cu(A)–S(3A)	91.69(3)	S(1B)–Cu(B)–S(3B)	88.39(3)
S(1A)–Cu(A)–S(1A)	180.00(9)	S(1B)–Cu(B)–S(1B)	179.9(1)
S(1A)–Cu(A)–S(2A)	88.14(3)	S(1B)–Cu(B)–S(2B)	91.45(3)
S(1A)–Cu(A)–S(3A)	88.31(3)	S(1B)–Cu(B)–S(3B)	91.61(3)
S(2A)–Cu(A)–S(3A)	87.92(3)	S(2B)–Cu(B)–S(3B)	87.91(3)
S(2A)–Cu(A)–S(2A)	179.86(3)	S(2B)–Cu(B)–S(2B)	180.0(1)
S(2A)–Cu(A)–S(3A)	92.08(3)	S(2B)–Cu(B)–S(3B)	92.09(3)
S(3A)–Cu(A)–S(3A)	179.88(3)	S(3B)–Cu(B)–S(3B)	179.9(1)
Cu(A)–S(1A)–C(1A)	97.6(1)	Cu(B)–S(1B)–C(1B)	98.5(1)
Cu(A)–S(1A)–C(6A)	101.6(1)	C(6B)–S(1B)–Cu(B)	102.8(1)
C(1A)–S(1A)–C(6A)	103.6(2)	C(6B)–S(1B)–C(1B)	103.4(2)
Cu(A)–S(2A)–C(2A)	103.0(1)	Cu(B)–S(2B)–C(2B)	101.7(1)
Cu(A)–S(2A)–C(3A)	98.7(1)	C(3B)–S(2B)–Cu(B)	98.1(1)
C(2A)–S(2A)–C(3A)	103.7(2)	C(3B)–S(2B)–C(2B)	103.2(2)
Cu(A)–S(3A)–C(4A)	103.6(1)	C(4B)–S(3B)–Cu(B)	102.8(1)
Cu(A)–S(3A)–C(5A)	98.8(1)	C(5B)–S(3B)–Cu(B)	97.9(1)
C(4A)–S(3A)–C(5A)	103.2(2)	C(4B)–S(3B)–C(5B)	102.9(2)
S(1A)–C(1A)–C(2A)	116.0(3)	S(1B)–C(1B)–C(2B)	116.5(3)
S(2A)–C(2A)–C(1A)	113.2(2)	S(2B)–C(2B)–C(1B)	113.4(3)
S(2A)–C(3A)–C(4A)	115.7(2)	C(4B)–C(3B)–S(2B)	116.1(3)
S(3A)–C(4A)–C(3A)	112.0(2)	C(3B)–C(4B)–S(3B)	112.9(2)
S(3A)–C(5A)–C(6A)	116.0(2)	C(6B)–C(5B)–S(3B)	115.6(2)
S(1A)–C(6A)–C(5A)	113.0(2)	C(5B)–C(6B)–S(1B)	112.5(2)
N(A)–C(8A)–C(7A)	179.7(9)	N(B)–C(8B)–C(7B)	179.7(7)
F(1A)–B(A)–F(2A)	109.1(3)	F(2B)–B(B)–F(1B)	109.2(3)
F(1A)–B(A)–F(3A)	108.4(3)	F(1B)–B(B)–F(3B)	108.9(3)
F(1A)–B(A)–F(4A)	109.5(3)	F(1B)–B(B)–F(4B)	109.0(3)
F(2A)–B(A)–F(3A)	109.8(3)	F(2B)–B(B)–F(3B)	110.8(3)
F(2A)–B(A)–F(4A)	109.2(3)	F(2B)–B(B)–F(4B)	109.9(3)
F(3A)–B(A)–F(4A)	110.7(3)	F(3B)–B(B)–F(4B)	109.1(3)

[a] Numbers in parentheses are e.s.d.s in the least significant digit.

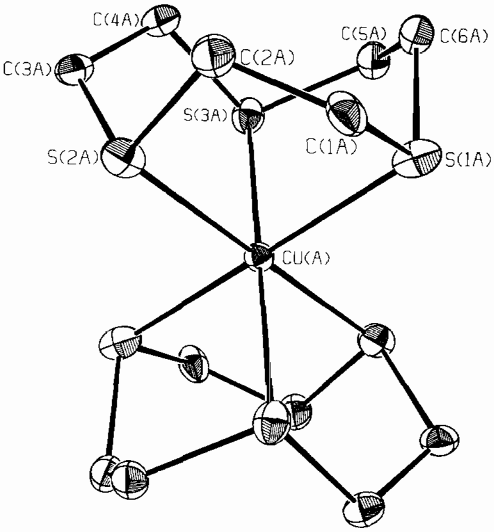

Fig. 1. ORTEP projection of the cation $Cu(ttcn)_2^{2+}$ in $Cu(ttcn)_2(BF_4)_2(MeCN)_2$ at 117 K with atomic numbering and 25% probability ellipsoids. The structures for unit A and B are the same within experimental error.

room temperature the crystal is in the orthorhombic space group *Pbca* [1] but on cooling to 117 K it changes to the monoclinic space group $P2_1/c$ which is observed at 117 K. The heat capacity measurements show a further change on cooling below 100 K which may coincide with a statically distorted CuS_6 core. Unfortunately we do not have access to X-ray structure determination at 4.2 K. The remarkable feature, however, is that the CuS_6 octahedra are hardly distorted even at 100 K.

Description of the structure of the cadmium compound 2

Coordination bond distances and angles for the cation are given in Table 8. A drawing of the cation $Cd(ttcn)_2^{2+}$ is given in Fig. 3. The cadmium atom is on a crystallographic inversion center and the CdS_6^{2+} core has slightly distorted octahedral geometry. The Cd–S bond lengths in this complex, 2.649–2.663 Å, are at the low end of the range for Cd(II)–thioether complexes, 2.663–2.82 Å [35–39]. The coordinated ttcn ligands are close in geometry to the uncoordinated ligand [40].

Description of the structure of the copper compound 3

Coordination bond distances and angles for the cation are given in Table 9. A drawing of the cation $Cu(ttcn)_2^{2+}$ is given in Fig. 4. The ttcn ligand acts as a tridentate ligand to the copper ion, but in dramatic contrast to the corresponding acetonitrile solvate, i.e. copper compound **1**, the CuS_6^{2+} core is substantially distorted from octahedral. This is clearly illustrated by the large difference of 0.16 Å between the maximum and minimum Cu–S bond lengths. (This CuS_6 distortion can also be pictured in the way described above for $Cu(ttcn)_2(BF_4)_2(MeCN)_2$. That is, by viewing down the axis through the copper atom and perpendicular to the two parallel planes each of which is defined by the three sulfur atoms in the same ttcn ligand. The dihedral angles between the sulfur atom of one ttcn ligand and the centers of the two planes and either *cis* sulfur atom

TABLE 7. Structural properties of bis(ttcn) metal compounds

Compound	M–S distances	S–M–S angles	Comments	Ref.
$Rh(ttcn)_2(Tf)_3$	2.331, 2.345, 2.345	not reported	octahedral	15
$Ru(ttcn)_2(PF_6)_3$	2.332, 2.334	88.8	octahedral	16
$Ru(ttcn)_2(Tf)_2$	2.331, 2.344	87.6, 87.8, 92.2, 92.4	octahedral	12
$Ru(ttcn)_2(BPh_4)_2(dmso)_2$	2.327, 2.336, 2.333	87.9, 88.1, 88.3	octahedral	13
$Pt(ttcn)_2(PF_6)_2$	2.25, 2.30 (2.88, 2.93)	88.1, 91.5 (84.0, 97.2)	square planar	8
$Co(ttcn)_2(BF_4)_2(MeNO_2)$	2.253, 2.580, 2.635	86.0...94.1	tetragonal	6
$Co(ttcn)_2(BF_4)_2(MeNO_2)_2$	2.240, 2.367, 2.356	88–92	near octahedral	1
$Co(ttcn)_2(ClO_4)_3$	2.249, 2.253, 2.258	89.3	octahedral	4
$Ni(ttcn)_2(BF_4)_2$	2.377, 2.380, 2.400	88–92	near octahedral	1
$Cu(ttcn)_2(BF_4)_2(MeCN)_2$	2.426, 2.459, 2.419	87.2, 92.8	near octahedral	1
$Cu_2(ttcn)_3(BF_4)_2(H_2O)$	2.238, 2.320	94.2, 122.1	tetrahedral	22
$Au(ttcn)_2(PF_6)_2$	2.350, 2.733, 2.825, 2.302	154, 113, 118.4, 156.4, 115.5, 110.8	distorted tetrahedral	21
$Pd(ttcn)(PF_6)_2$	2.333, 2.318, (2.957)	83–97	tetragonal	7
$Pd(ttcn)_2(PF_6)_2(H_2O)$	2.309, 2.314, (3.005)	82–98	tetragonal	5
$Pd(ttcn)_2(ClO_4)_4(H_3O)(H_2O)_3$	2.545, 2.356, 2.369	87.3, 87.2, 88.9	tetragonal	10
$Fe(ttcn)_2(PF_6)_2$	2.241, 2.251, 2.259	89.2–90.8	octahedral	3
$Fe(ttcn)_2(ClO_4)_3$	2.280, 2.285, 2.276	90.0, 90.2, 89.7	octahedral	23
$Hg(ttcn)_2(PF_6)_2(H_2O)_{1/3}$	2.638, 2.728, 2.712	82.6, 81.0, 82.9	octahedral (tetragonal compression)	20
$Ag(ttcn)_2(Tf)$	2.753, 2.727, 2.696	80.5, 80.1, 100.7, 79.3, 99.5, 99.9	octahedral (trigonal elongation)	25
$Ag_3(ttcn)_3Ag(ttcn)_2(ClO_4)_4$	2.753, 2.691	90.1, 79.6, 116.0, 159.7, 78.6	distorted octahedral	14
$Au(ttcn)_2(H_3O)(ClO_4)_4(H_2O)_3$	2.926, 2.348, 2.354	not reported	distorted octahedral	21
$Cd(ttcn)_2(BF_4)_2(MeNO_2)_2$	2.649, 2.650, 2.663	83–97	octahedral	this work
$Cu(ttcn)_2(BF_4)_2(MeCN)_2$	2.407–2.458	86–94	octahedral (117 K)	this work
$Cu(ttcn)_2(BF_4)_2(MeNO_2)_2$	2.343, 2.487, 2.504	87–93	tetragonal	this work

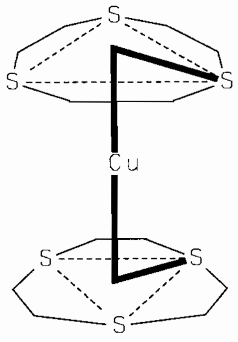

Fig. 2. Dihedral angle about the pseudo C_3 axis perpendicular to the intraligand S,S,S planes.

of the other ligand and the centers of the two planes differs from 60° by 0.4–3.7°.) This expected Jahn–Teller distortion is observed at room temperature and heat capacity measurements between room temperature and 4 K show no phase transitions. Hence solvation with acetonitrile instead of nitromethane results in an enormous difference in the temperature at which the static Jahn–Teller effect manifests itself. Although lattice forces resulting in this observation are not understood, such effects have been reported before [27]. In an attempt to identify these intermolecular interactions a search of intermolecular non-bonded interactions was made in $Cu(ttcn)_2(BF_4)_2(MeCN)_2$ and $Cu(ttcn)_2(BF_4)_2(MeNO_2)_2$. Only one such contact significantly less than the sum of the van der Waals radii of the respective atoms was found. In both molecule A and B of $Cu(ttcn)_2(BF_4)_2(MeCN)_2$, there is in each $Cu(ttcn)_2^{2+}$ unit and its nearest two symmetry related MeCN molecules two $S\cdots N$ symmetry equivalent distances of 3.339(3) and 3.340(3) Å, respectively, in A and B. These distances are significantly less than the sum of the van der Waals radii for S and N (3.35 Å). However, the significance of this observation remains to be established.

Comparison of the $Cu(ttcn)_2^{2+}$ cation in the $Cu(ttcn)_2(BF_4)_2(MeNO_2)_2$ complex (**3**) with that in the $Cu(ttcn)_2(BF_4)_2(MeCN)_2$ complex (**1**) at room temperature reveal the way in which Jahn–Teller distortion is achieved. The ttcn ligands in both complexes are

TABLE 8. Bond lengths (Å) and bond angles in $Cd(ttcn)_2(BF_4)_2(MeNO_2)_2$

Bond distances (Å)[a]			
Cd–S1	2.663(1)	F2–B	1.305(5)
Cd–S2	2.650(1)	F3–B	1.276(5)
Cd–S3	2.649(1)	F4–B	1.228(5)
S1–C1	1.811(3)	O1–N	1.228(7)
S1–C6	1.806(4)	O2–N	1.100(6)
S2–C2	1.800(3)	N–C	1.408(6)
S2–C3	1.814(3)	C1–C2	1.538(5)
S3–C4	1.814(4)	C3–C4	1.507(6)
S3–C5	1.814(3)	C5–C6	1.517(5)
F1–B	1.301(5)		
Bond angles (°)[a]			
S1–Cd–S1	180	C4–S3–C5	103.4(2)
S1–Cd–S2	83.01(2)	O1–N–O2	125.6(7)
S1–Cd–S2	96.99(2)	O1–N–C	114.6(5)
S1–Cd–S3	82.96(2)	O2–N–C	119.8(7)
S1–Cd–S3	97.04(2)	S1–C1–C2	114.0(2)
S2–Cd–S2	180	S2–C2–C1	117.4(2)
S2–Cd–S3	83.13(3)	S2–C3–C4	115.5(3)
S2–Cd–S3	96.87(3)	S3–C4–C3	118.6(2)
S3–Cd–S3	180	S3–C5–C6	115.2(2)
Cd–S1–C1	102.1(1)	S1–C6–C5	118.2(2)
Cd–S1–C6	96.8(1)	F1–B–F2	111.5(4)
C1–S1–C6	103.4(2)	F1–B–F3	113.8(5)
Cd–S2–C2	97.1(1)	F1–B–F4	110.3(5)
Cd–S2–C3	102.6(1)	F2–B–F3	106.1(4)
C2–S2–C3	103.3(2)	F2–B–F4	111.3(6)
Cd–S3–C4	97.6(1)	F3–B–F4	103.5(6)
Cd–S3–C5	102.6(1)		

[a] Numbers in parentheses are e.s.d.s in the least significant digits.

TABLE 9. Bond lengths (Å) and bond angles (°) in $Cu(ttcn)_2(BF_4)_2(MeNO_2)_2$

Bond distances (Å)[a]			
Cu–S1	2.504(2)	C3–C4	1.51(1)
Cu–S2	2.343(2)	C5–C6	1.497(9)
Cu–S3	2.487(2)	B–F1	1.31(1)
S1–C1	1.833(8)	B–F2	1.31(1)
S1–C6	1.834(7)	B–F3	1.25(1)
S2–C2	1.821(7)	B–F4	1.33(1)
S2–C3	1.818(7)	C7–N	1.42(1)
S3–C4	1.825(6)	N–O1	1.22(1)
S3–C5	1.792(7)	N–O2	1.18(1)
C1–C2	1.52(1)		
Bond angles (°)[a]			
S1–Cu–S1	180	C4–S3–C5	102.8(4)
S1–Cu–S2	88.32(7)	S1–C1–C2	116.0(5)
S1–Cu–S2	91.68(7)	S2–C2–C1	112.2(5)
S1–Cu–S3	93.02(6)	S2–C3–C4	116.1(5)
S1–Cu–S3	86.98(6)	S3–C4–C3	111.2(5)
S2–Cu–S2	180	S3–C5–C6	117.7(5)
S2–Cu–S3	91.95(6)	S1–C6–C5	113.3(5)
S2–Cu–S3	88.05(6)	F1–B–F2	110.8(9)
S3–Cu–S3	180	F1–B–F3	104(1)
Cu–S1–C1	95.7(3)	F1–B–F4	102.6(9)
Cu–S1–C6	101.2(2)	F2–B–F3	116(1)
C1–S1–C6	104.1(4)	F2–B–F4	112.6(9)
Cu–S2–C2	105.2(3)	F3–B–F4	110(1)
Cu–S2–C3	99.4(2)	C7–N–O1	114(1)
C2–S2–C3	104.5(4)	C7–N–O2	121(1)
Cu–S3–C4	101.5(2)	O1–N–O2	124(1)
Cu–S3–C5	98.2(2)		

[a] Numbers in parentheses are e.s.d.s in the least significant digits.

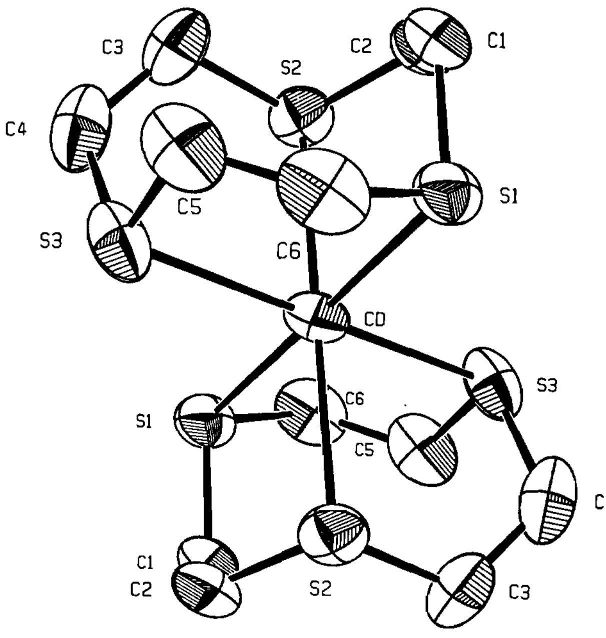

Fig. 3. ORTEP projection of the cation $Cd(ttcn)_2^{2+}$ in $Cd(ttcn)_2(BF_4)_2(MeNO_2)_2$ with numbering and 25% probability ellipsoids.

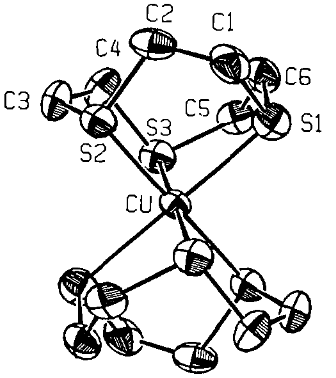

Fig. 4. ORTEP projection of $Cu(ttcn)_2(BF_4)_2(MeNO_2)_2$ at room temperature with atomic numbering and 25% probability ellipsoids.

remarkably similar to each other in geometry. However, in **3** there is a twist of the ligands relative to each other resulting in two shortened, two elongated and two essentially unchanged Cu–S bond lengths as shown in Table 7 relative to **1**. The slight changes in the geometry of the ttcn ligands of **3** relative to **1** are incremental and best revealed by the intraligand S···S distances which differ by 0.08 Å in **3** but by only 0.02

Å in 1*. On the other hand, the interligand S···S distances in the $Cu(ttcn)_2^{2+}$ unit differ by 0.15 Å in **3** but by 0.06 Å in **1**. Thus tetragonal distortion in the cation is achieved not by significantly changing the conformational geometry of the individual ttcn molecules but by twisting the ligands each as a whole relative to each other and the metal atom [33]. To be sure, the geometry of the ligand can change, as illustrated most dramatically in the bridging ttcn ligand in the $Cu_2(ttcn)_3^{2+}$ complex [22]. What is remarkable is the apparent reluctance of the ttcn ligand to distort. The relative energies of the various conformational minima for ttcn are unknown but MM1 calculations suggested that the observed [333] twist boat chair conformation and the [1222] conformation with a C_2 axis should be the lowest energy conformers [41]. Indeed the calculations suggested that the [1222] conformer is lower in energy than the [333] conformer, but photoelectron spectroscopic [41] and X-ray crystallographic [40] analysis show that this is not the case in the gas phase or solid state. Nevertheless these results are of interest in light of the structure of the bridging ligand in $Cu_2(ttcn)_3^{2+}$ which approximates [1222] conformation.

Because Jahn–Teller distortion in **3** is achieved primarily by twisting ttcn units relative to each other rather than by distortion of each unit we reexamined the structure of $Co(ttcn)_2(BF_4)_2(MeNO_2)_2$ (**4**)**. It has been suggested [32] that the 0.12 Å difference in bond lengths in this compound requires that the ligand unit itself distort. As shown in Table 10 the intraligand S···S distances in this complex differ by only 0.05 Å but the interligand distances differ by 0.13 Å. However, there are also significant geometry changes in the ttcn ligands in this complex relative to those of **1** and **3**. The average of the two different CSCC and SCCS dihedral angles for the ttcn ligand in the cobalt complex are −135, 51 and 64°, respectively, but −132, 58 and 56°, respectively, for the copper complexes. Thus Jahn–Teller distortion in this complex occurs by both ligand distortion and twisting of the ligands relative to each other.

In conclusion, Jahn–Teller distortion may be achieved in metal bis (ttcn) complexes by either twisting the ligand units relative to each other or by distorting the ligand units. In **3** distortion is achieved predominantly by twisting and in **4** by twisting and ligand distortion. It appears that the means by which Jahn–Teller distortion is achieved results from a complex interplay of factors including a contribution from the energy required to distort the ttcn ligand.

Spectral information

The IR spectra of the several ttcn compounds are very similar in line shapes and relative intensities throughout the series Co, Ni, Cu, Fe, Cd, indicating a similar ligand conformation for all compounds [42].

EPR powder spectra are recorded for the pure copper compound (at 300, 77 and 4 K), for the Cu(II) dope in $Fe(ttcn)_2(BF_4)_2$ (at 300 and 77 K at X-band and at Q-band frequencies). The results are summarized in Table 11, and compared with the published data [27] for the perchlorate salts in frozen dmso solution. As can be seen from the Table, the parameters agree with

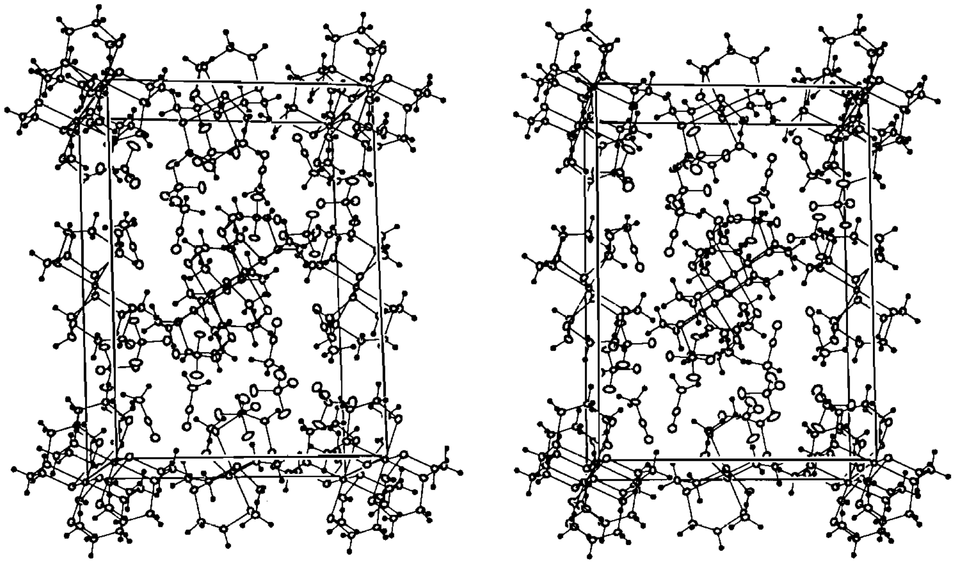

Fig. 5. ORTEP projection of the unit cell of $Cu(ttcn)_2(BF_4)_2(MeCN)_2$ at 117 K.

---

*The S···S distance in the free ligand is 3.45 Å [40].

**Although the table of geometric parameters published for this structure are correct [1], the negative sign for the x atomic coordinate for S(1) is missing in the table of fractional atomic coordinates for this complex, i.e. for atom S(1) in Table 4 the x coordinate is −0.0047.

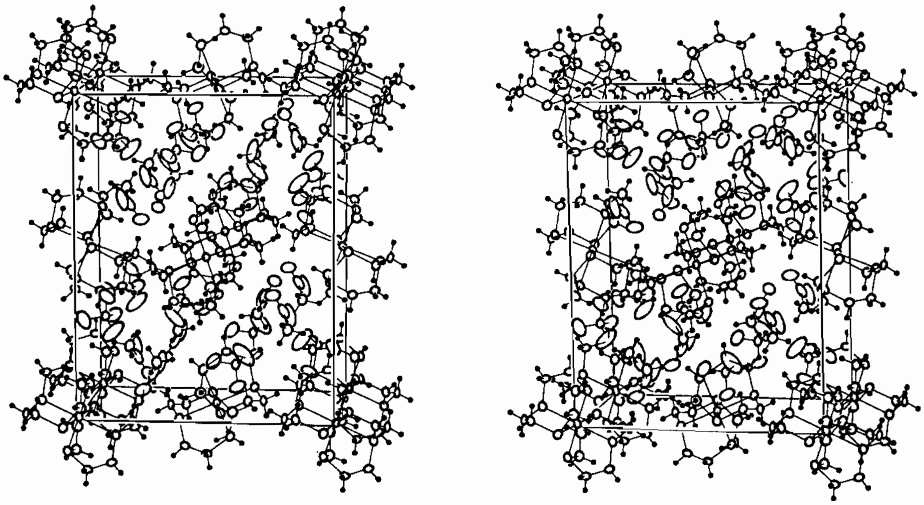

Fig. 6. ORTEP projection of the unit cell of $Cu(ttcn)_2(BF_4)_2(MeNO_2)_2$ at room temperature.

TABLE 10. Comparison of S···S distances in $Cu(ttcn)_2(BF_4)_2(MeCN)_2$ (**1**), $Cu(ttcn)_2(BF_4)_2(MeNO_2)_2$ (**3**) and $Co(ttcn)_2(BF_4)_2(MeNO_2)_2$ (**4**)

Compound	Intraligand S···S distances (Å)	Interligand S···S distances (Å)	Ref.
$Cu(ttcn)_2(BF_4)_2(MeCN)_2$ (**1**)	3.37, 3.37, 3.39	3.48, 3.51, 3.54	1
$Cu(ttcn)_2(BF_4)_2(MeNO_2)_2$ (**3**)	3.36, 3.38, 3.44	3.47, 3.48, 3.62	this work
$Co(ttcn)_2(BF_4)_2(MeNO_2)_2$ (**4**)	3.24, 3.24, 3.29	3.26, 3.27, 3.39	2

TABLE 11. EPR spectroscopic data of $Cu(ttcn)_2^{2+}$ species

Compound[a]	$g_\parallel$	A values (Gauss)	$g_\perp$	A values (Gauss)
$Cu(ttcn)_2$ powder[b]			2.06 (isotropic)	
$Cu(ttcn)_2$ solution[c]	2.114	153[e]	2.027[e]	
$Cd(ttcn)_2$ powder[d]	2.117	150[e]	2.045	20[e]
			2.029	28[e]
$Cd(ttcn)_2$ single crystal[d]	2.06 (along 3-fold axis)	70[f]		
$Fe(ttcn)_2$ powder[d]	2.113	153^3	2.035 and 2.025 (rhombic)	

[a] Only the cationic part of the molecule is given. [b] As the perchlorate and tetrafluoroborate, at 77 and 4 K; no effects seen of the lattice solvent. [c] Frozen DMSO solution at 130 K [27]. [d] Cu(II) doped compound at 77 K (X-band and Q-band). The listed rhombic splitting was resolved only at Q-band. [e] Error about 3–5 G. [f] Rotations around several crystal axes showed as extreme values for $A_\parallel$ 152 Gauss at $g_\perp = 2.10$ and the values given in the Table for non-rotation sensitive orientations.

each other. At room temperature the doped compounds contain Cu(II) ions which occur partly in dynamic and statically distorted CuS_6 chromophores. Upon cooling all ions take the typical tetragonally elongated geometry [43].

Electrochemistry of $Cu(ttcn)_2^{2+}$

The cyclic voltammetry for $Cu(ttcn)_2^{2+}$ in aqueous pH 3 solution yields a reversible current–voltage curve with well-defined cathodic and anodic peaks. Data were obtained from 5 mV/s to 20 V/s and agreement between theory and experiment was excellent. From the curve fitting over the specified scan rate range, a heterogeneous electron transfer rate constant of $k_{sh} = 1.3 \times 10^{-2} \pm 0.001$ cm s^{-1} ($\alpha = 0.45 \pm 0.04$) and $E^{0\prime} = 0.408 \pm 0.002$ V versus AgCl/Ag reference were obtained. By contrast the approximate $E^{0\prime}$ for the free Cu(II)/Cu(I) couple in the same medium was below

0.12 V. The resulting positive potential shift on complex formation is indicative of the preferential stabilization of Cu(I) by about ten orders of magnitude. Controlled potential electrolysis of the yellow $Cu(ttcn)_2^{2+}$ in aqueous carbonate buffer pH 6 yields a colorless solution and a one-electron reduction as determined by controlled potential coulometry. No other redox processes were observed in this medium. As expected, the cyclic voltammetry of the product solution was similar to that of the original solution which could be completely regenerated by electrochemical oxidation. The electronic spectral data for this $Cu(ttcn)_2^{2+}$ in solution are λ_{max} 340 (54 l mol^{-1} cm^{-1}), 430 (50 l mol^{-1} cm^{-1}) nm. Current voltage curves obtained at a rotating disk electrode are further consistent with the diffusion-controlled one-electron reduction of the Cu(II) complex. Further details concerning the electrochemistry of this system are given elsewhere [44].

Determination of formation constants

Spectrophotometric data were used to determine the two successive formation constants for the copper ttcn complex in water. A gradient search method [45] was used to determine the best fit for the variation of the complex absorbance with total ligand concentration. The results of these calculations are $K_1 = 9 \times 10^4$, $K_2 = 2 \times 10^6$, $K_3 = K_1K_2 = 1.8 \times 10^{11}$. These formation constants are two orders of magnitude greater than values reported for all previous thioether donor systems [46], indicating the advantages of preorganization in this ligand.

Supplementary material

Tables of final hydrogen atom positional and thermal parameters; tables of anisotropic temperature factors; listings of structure factor amplitudes for compounds **1**–**3** are available from the authors on request.

Acknowledgements

The authors are indebted to Mr S. Sorter for assistance with the data collection, to Professor W. J. A. Maaskant and Mr P. J. A. Wijnands for helpful discussions and to the Strategic Metals Recovery Research Facility at the University of Arizona for ICP-AES analysis of the Cu-doped $Cd(ttcn)_2(BF_4)_2(MeNO_2)_2$. The authors thank the Molecular Structure Laboratory of the University of Arizona for determining the X-ray crystal structures of **2** and **3** and Dr E. Bonjour of the Centre d'Études Nucléaire de Grenoble for the heat capacity measurements on **1** and **3**. The authors thank Sanaullah and Kenji Kano for assistance with the electrochemical measurements. R.S.G., L.K.S., D.D.S., and G.S.W. gratefully acknowledge support of this work by the US Public Health Service, National Institutes of Health, Grant No. HL 15104.

References

1 W. N. Setzer, C. A. Ogle, G. S. Wilson and R. S. Glass, *Inorg. Chem., 22* (1983) 266.

2 M. T. Ashby and D. L. Lichtenberger, *Inorg. Chem., 24* (1985) 636.

3 K. Wieghardt, H.-J. Küppers and J. Weiss, *Inorg. Chem., 24* (1985) 3067.

4 H.-J. Küppers, A. Neves, C. Pomp, D. Ventur, K. Wieghardt, B. Nuber and J. Weiss, *Inorg. Chem., 25* (1986) 2400.

5 K. Wieghardt, H.-J. Küppers, E. Raabe and C. Kruger, *Angew. Chem., Int. Ed. Engl., 25* (1986) 1101.

6 J. R. Hartmann, E. J. Hintsa and S. R. Cooper, *J. Am. Chem. Soc., 108* (1986) 1208.

7 A. J. Blake, A. J. Holder, T. I. Hyde, Y. V. Roberts, A. J. Lavery and M. Schröder, *J. Organomet. Chem., 323* (1987) 261.

8 A. J. Blake, R. O. Gould, A. J. Holden, T. I. Hyde, A. J. Lavery, M. O. Odulate and M. Schröder, *J. Chem. Soc., Chem. Commun.,* (1987) 118.

9 J. Clarkson, R. Yagbasan, P. J. Blower, S. C. Rawle and S. R. Cooper, *J. Chem. Soc., Chem. Commun.,* (1987) 950.

10 A. J. Blake, A. J. Holder, T. I. Hyde and M. Schröder, *J. Chem. Soc., Chem. Commun.,* (1987) 987.

11 H.-J. Küppers, K. Wieghardt, B. Nuber, J. Weiss, E. Bill and A. X. Trautwein, *Inorg. Chem., 26* (1987) 3762.

12 S. C. Rawle, T. J. Sewell and S. R. Cooper, *Inorg. Chem., 26* (1987) 3769.

13 M. N. Bell, A. J. Blake, M. Schröder, H.-J. Küppers and K. Wieghardt, *Angew. Chem., Int. Ed. Engl., 26* (1987) 250.

14 H.-J. Küppers, K. Wieghardt, Y.-H. Tsay, C. Krüger, B. Nuber and J. Weiss, *Angew. Chem., Int. Ed. Engl., 26* (1987) 575.

15 S. C. Rawle, R. Yagbasan, K. Prout and S. R. Cooper, *J. Am. Chem. Soc., 109* (1987) 6181.

16 A. J. Blake, R. O. Gould, A. J. Holder, T. I. Hyde and M. Schröder, *J. Chem. Soc., Dalton Trans.,* (1988) 1861.

17 C. Pomp, S. Drücke, H.-J. Küppers, K. Wieghardt, C. Krüger, B. Nuber and J. Weiss, *Z. Naturforsch., Teil B, 43* (1988) 299.

18 E. W. Abel, P. D. Beer, I. Moss, K. G. Orrell, V. Sik, P. A. Bates and M. B. Hursthouse, *J. Organomet. Chem., 341* (1988) 559.

19 A. J. Blake, A. J. Holder, Y. V. Roberts and M. Schröder, *Acta Crystallogr., Sect. C, 44* (1988) 360.

20 A. J. Blake, A. J. Holder, T. I. Hyde, G. Reid and M. Schröder, *Polyhedron,* (1989) 2041.

21 A. J. Blake, R. O. Gould, J. A. Greig, A. J. Holder, T. I. Hyde and M. J. Schröder, *J. Chem. Soc., Chem. Commun.,* (1989) 876.

22 J. A. Clarkson, R. Yagbasan, P. J. Blower and S. R. Cooper, *J. Chem. Soc., Chem. Commun.,* (1989) 1244.

23 A. J. Blake, A. J. Holder, T. I. Hyde and M. Schröder, *J. Chem. Soc., Chem. Commun.,* (1989) 1433.

24 H. Elias, G. Schmidt, H.-J. Küppers, M. Saher, K. Wieghardt, B. Nuber and J. Weiss, *Inorg. Chem., 28* (1989) 3021.

25 P. J. Blower, J. A. Clarkson, S. C. Rawle, J. R. Hartman, R. E. Wolf, Jr., R. Yagbasan, S. G. Bott and S. R. Cooper, *Inorg. Chem., 28* (1989) 4040.

26 A. J. Blake, R. D. Crofts, G. Reid and M. Schröder, *J. Organomet. Chem., 359* (1989) 371.
27 D. Reinen, A. Ozarowski, B. Jakob, J. Pebler, H. Stratemeier, K. Wieghardt and F. Tolksdorf, *Inorg. Chem., 26* (1987) 4010.
28 A. J. Kinneging and R. G. A. de Graaff, *J. Appl. Crystallogr., 17* (1984) 364.
29 B. A. Frenz, in H. Schenk, R. Olthof-Hazelkamp, R. von Konigsveld and G. D. Bassi (eds.), *Computing in Crystallography,* Delft University, Netherlands, 1978, pp. 64–71.
30 D. L. Langhus and G. S. Wilson, *Anal. Chem., 51* (1979) 1139.
31 K. Kano, unpublished results, 1991.
32 S. R. Cooper and S. C. Rawle, *Struct. Bonding (Berlin), 72* (1990) 1.
33 J. C. A. Boeyens, S. M. Dobson and R. D. Hancock, *Inorg. Chem., 24* (1985) 3073.
34 P. E. M. Wijnands, *Ph.D. Thesis,* Leiden University, 1989.
35 S. H. Whitlow, *Acta Crystallogr., Sect. B, 31* (1975) 2531.
36 T. C. Mak, W.-H. Yip, G. Smith, E. J. O'Reilly and C. H. L. Kennard, *Inorg Chim. Acta, 84* (1984) 57.
37 F. H. Herbstein, P. Ashkenazi, M. Kaftory, M. Kapon, G. M. Reisner and D. Ginsburg, *Acta Crystallogr., Sect. B, 42* (1986) 575.
38 W.-H. Chan, T. C. W. Mak, W. H. Yip and C. H. L. Kennard, *Polyhedron, 5* (1987) 881.
39 G. Smith, E. J. O'Reilly, C. H. L. Kennard, T. C. W. Mak, W.-H. Yip and W. H. Chan, *Aust. J. Chem., 41* (1988) 1769.
40 R. S. Glass, G. S. Wilson and W. N. Setzer, *J. Am. Chem. Soc., 102* (1980) 5068.
41 W. N. Setzer, B. R. Coleman, G. S. Wilson and R. S. Glass, *Tetrahedron, 37* (1981) 2743.
42 K. Nakamoto, *Infrared and Raman Spectra of Inorganic and Coordination Compounds,* Wiley, New York, 3rd edn., 1978.
43 B. J. Hathaway and D. E. Billing, *Coord. Chem. Rev., 5* (1970) 143.
44 Sanaullah, K. Kano, R. S. Glass and G. S. Wilson, *J. Am. Chem. Soc., 115* (1993) 592.
45 P. R. Bevington, *Data Reduction and Error Analysis for the Physical Sciences,* McGraw-Hill, New York, 1969.
46 S. G. Murray and F. R. Hartley, *Chem. Rev., 81* (1981) 365.